Perforated nanocap array: Facile fabrication process and efficient surface enhanced Raman scattering with fluorescence suppression*

Wang Jun(王 军), Huang Li-Qing(黄丽清)†, Tong Hui-Min(童慧敏),
Zhai Li-Peng(翟立鹏), Yuan Lin(袁 林), Zhao Li-Hua(赵丽华),
Zhang Wei-Wei(张薇薇), Shan Dong-Zhi(单冬至), Hao Ai-Wen(郝爱文), and Feng Xue-Hong(冯雪红)

Non-equilibrium Condensed Matter and Quantum Engineering Laboratory, School of Science, Xi'an Jiaotong University, Xi'an 710049, *China*

(Received 3 August 2012; revised manuscript received 24 September 2012)

Recently, individual reduced-symmetry metal nanostructures and their plasmonic properties have been studied extensively. However, little attention has been paid to the approach to fabricating ordered reduced-symmetry metal nanostructure arrays. In this paper, a novel perforated silver nanocap array with high surface-enhanced Raman scattering (SERS) activity and fluorescence suppression is reported. The array is fabricated by electron beam evaporating Ag onto the perforated barrier layer side of a hard anodization (HA) anodic aluminum oxide (AAO) template. The morphology and optical property of the perforated silver nanocap array are characterized by an atomic force microscope (AFM), a scanning electron microscope (SEM), and absorption spectra. The results of SERS measurements reveal that the perforated silver nanocap array offers high SERS activity and fluorescence suppression compared with an imperforated silver nanocap array.

Keywords: reduced-symmetry structures, perforated nanocap array, surface-enhanced Raman scattering, anodic aluminum oxide

PACS: 73.22.Gk, 73.20.Mf **DOI:** 10.1088/1674-1056/22/4/047301

1. Introduction

Recently, reduced-symmetry metal nanostructures including three-dimensional nanocup/nanocaps,[1–3] perforated semi-shells,[4,5] crescent-moons,[6] and two-dimensional (2D) rings/disks[7] have attracted increasing interest. Numerous research efforts have been made to discover unique optical properties of these reduced-symmetry nanostructures, such as strong directionality of scattered light,[2] high structural resonance tunability,[4,7] and large electromagnetic field enhancement.[4–6] The promising large electromagnetic field enhancement provided by these nanostructures has been extensively used in high spatial resolution surface-enhanced Raman scattering (SERS) spectroscopy and imaging.[6] However, up to now, little attention has been paid to the approach to fabricating reduced-symmetry metal nanostructure arrays, especially perforated nanocap arrays, although the properties of individual reduced-symmetry metal nanostructures have been studied extensively.[3–7] The anodic aluminum oxide (AAO) template-based approach is a well-known method of fabricating ordered metal nanostructure arrays due to the AAO template long-range ordering, facile controllability, excellent reproducibility, easy fabrication, and modest cost.[8] AAO template-based metal nanopore,[9] nanoparticle,[10–12] nanowire,[13] and nanocap[14] array SERS-active substrates have been reported. However, the local electromagnetic fields and SERS activities of those nanostructure arrays were mainly increased by gap effect[11–16] (also called inter-particle coupling effect), which displayed a mechanism significantly different from the reduced-symmetry effect. In this paper, we report on a facile fabrication process for forming imperforated and perforated silver nanocap arrays by using an AAO template-based approach. The perforated silver nanocap array possesses both reduced-symmetry and ordered morphological characteristics. The optical properties and SERS activity of the as-fabricated perforated silver nanocap array are further investigated. The results of SERS measurements reveal that the perforated silver nanocap array offers high SERS activity and fluorescence suppression compared with imperforated silver nanocap array.

2. Experiment detail

2.1. Synthesis of template and silver nanocap arrays

The schematic plot for the fabrication of perforated silver nanocap array is shown in Fig. 1. The porous anodic aluminum oxide template was prepared by a two-step hard anodization (HA) technique in 0.3-M oxalic acid solutions at 130 V and −1.5 °C, followed by removing residual aluminum in a saturated $HgCl_2$ solution. The schematic cross sections of HA AAO template with and without aluminum are shown in Figs. 1(a) and 1(b), respectively. The perforated HA AAO template (the schematic cross section is shown in Fig. 1(c)) was obtained by etching barrier layer of HA AAO template in a 10-wt% H_3PO_4 solution at 30.0 °C for 50 min. Both imperforated and perforated silver nanocap arrays were fabricated by

*Project supported by the Industry Key Technologies R & D Project in Shaanxi Province of China (Grant No. 2012K07-19).
†Corresponding author. E-mail: lqhuangxjtu@126.com
© 2013 Chinese Physical Society and IOP Publishing Ltd

electron beam evaporating 200-nm thickness Ag onto the barrier sides of imperforated and perforated HA AAO templates, respectively, at a rate of 0.2 nm/s and a vacuum pressure of approximately 3×10^{-3} Pa. The schematic cross sections of imperforated and perforated silver nanocap arrays are shown in Figs. 1(d) and 1(e), respectively.

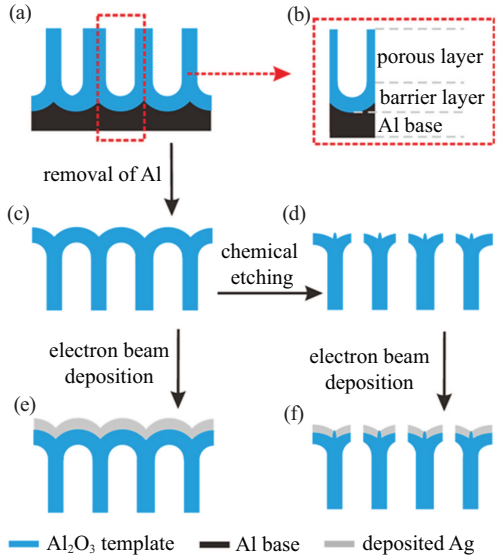


Fig. 1. (color online) Schematic plot for the fabrication of perforated silver nanocap array. (a) Fabricating HA AAO template with aluminum base by HA technique. The inset shows the corresponding cell structure. (b) Removing residual aluminum in a saturated $HgCl_2$ solution. (c) Perforating barrier layer of HA AAO template by wet chemical method. (d) and (e) Evaporating Ag onto the barrier layer sides of imperforated and perforated HA AAO templates, respectively.

2.2. Characterization

An atomic force microscope (AFM) with its tip in tap-mode (Micro-Nano D3000) and a scanning electron microscope (SEM, JOEL JSM-6700F) were employed to characterize the surface morphologies of templates and silver nanocap arrays. Optical absorption spectra were measured using a UV spectrophotometer (PerkinElmer Lambda 750S). Raman and SERS spectral measurements were carried out with a confocal Raman spectrometer (Horiba Jobin Yvon HR800) with 514-nm excitations. Rhodamine 6G (R6G) was adopted as the analyte for SERS measurement. The SERS-active substrate based imperforated and perforated silver nanocap arrays were immersed in 10^{-5}-M/L R6G ethanol solution for 2 h and then thoroughly rinsed with deionized water to ensure the same surface coverages for monolayer R6G molecules adsorbed onto different substrates.[12]

3. Result and discussion

3.1. Barrier layer morphological difference between imperforated and perforated HA AAO template

The barrier layer morphologies of imperforated and perforated HA AAO templates are shown in Fig. 2. As shown in Figs. 2(a) and 2(b), the barrier layer of imperforated HA AAO is a periodic array composed of close-packed hemispherical domes and could be described as an AAO nanocap array. The height of AAO nanocap is about 130 nm–150 nm and the array period is about 250 nm (as determined by SEM and AFM images). In contrast, the barrier layer morphology of the perforated HA AAO template is significantly different from that of imperforated one. As shown in Figs. 2(c) and 2(d),the perforated barrier layer is a periodic array composed of close-packed special cells, which combine a hexagonal ridge-like

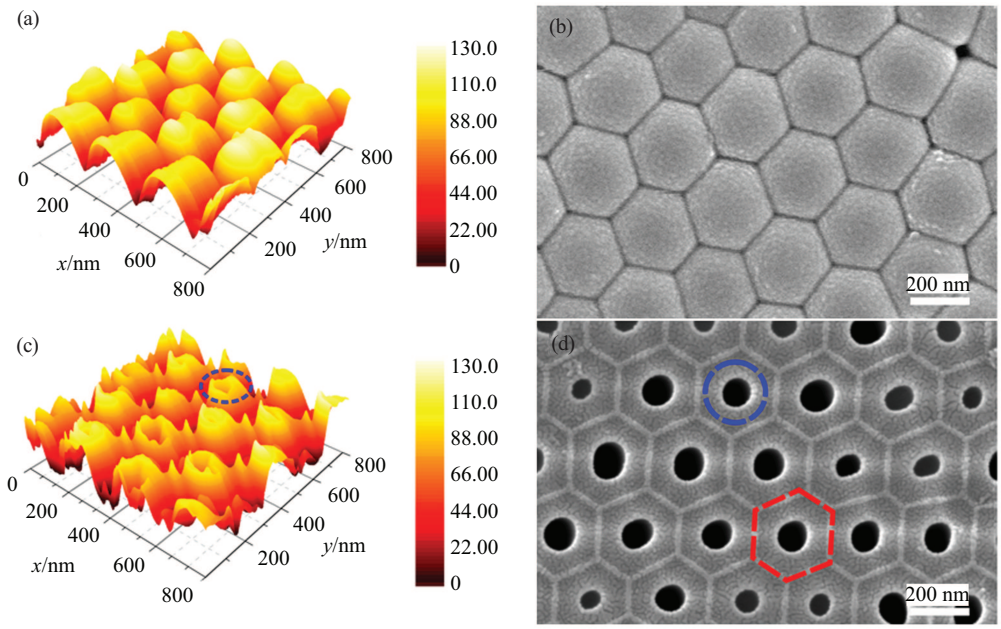


Fig. 2. (color online) AFM and SEM images of imperforated (a) and (b) and perforated (c) and (d) HA AAO templates. The circle indicates perforated hemispherical dome and the hexagon denotes a hexagonal ridge-like cell wall.

cell wall (marked with a hexagon) surrounding the perforated hemispherical dome (marked with a circle). These complex morphological characteristics can be ascribed to alumina composition and etching rate difference between barrier layer centre and boundary.[17,18] As a consequence, one can expect that the perforated HA AAO template will provide potential to fabricate perforated metal nanocap arrays with special optical property and SERS activity.

3.2. Morphology and optical properties of imperforated and perforated silver nanocap arrays

Imperforated and perforated silver nanocap arrays are obtained by electron beam evaporating Ag onto the imperforated and perforated barrier layer sides of HA AAO template and their SEM images are shown in Figs. 3(a) and 3(b), respectively. Comparing the morphologies of two types of silver nanocap arrays in Figs. 3(a) and 3(b), the effect of template morphology on the deposited silver distribution is verified.

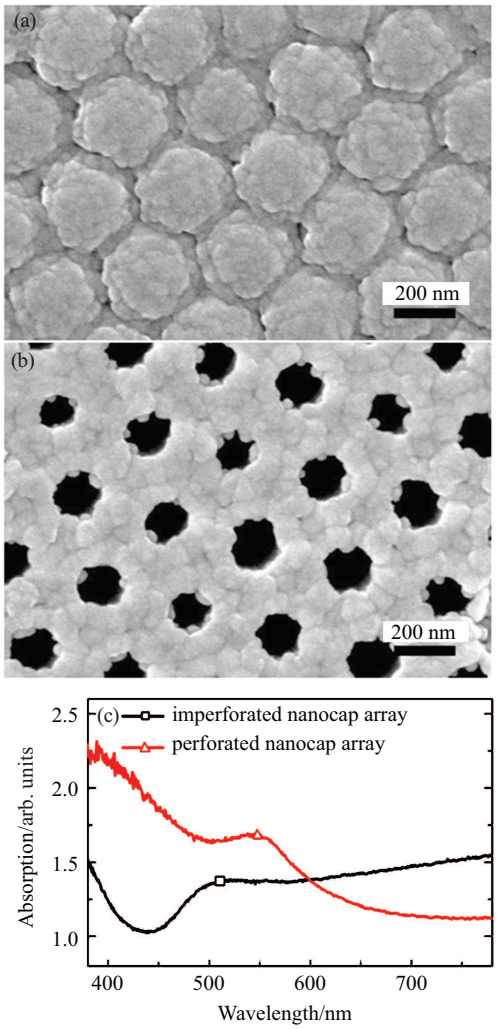


Fig. 3. (color online) Morphologies and optical properties of imperforated and perforated silver nanocap arrays with 200-nm thickness silver deposition. Panels (a) and (b) show the SEM images of imperforated and perforated silver nanocap arrays, respectively. Panel (c) displays the absorption spectra of imperforated (curve with square) and perforated silver nanocap arrays (curve with triangle).

As shown in Fig. 3(b), although coalescence of silver particles flattens hexagonal ridge-like cell wall but the perforated hemispherical domes are observed on the perforated nanocap array. Figure 3(c) demonstrates that the optical absorption peak of the perforated nanocap array is red-shifted significantly compared with that of the imperforated nanocap array, which resembles the red-shifting phenomenon of an individual perforated semi-shell nanostructure.[4] To further verify that the surface composition of the as-prepared nanocap array is silver, energy dispersive X-ray spectroscopy (EDS) analysis was applied and the result is shown in Fig. (a1) (See item (a1) in Appendix A).

3.3. SERS activity of imperforated and perforated silver nanocap arrays

SERS spectra of R6G adsorbed on imperforated and perforated silver nanocap arrays were measured using a 514-nm laser, and the measured results are shown in Fig. 4(a). The pronounced Raman bands in all SERS spectra at 1126, 1183, 1310, 1364, 1507, and 1648 cm^{-1} are observed, which match well with the reported results in Ref. [19]. Figure 4(a) indicates that the SERS intensity of R6G molecules absorbed into perforated nanocap array is much higher than that of imperforated nanocap array, in spite of the facts that the surface area and the corresponding number of absorbed R6G molecules for perforated nanocap array are smaller than those for imperforated silver nanocap array. The better SERS enhancement on perforated silver nanocap array can be attributed to the enhancement of intense local electromagnetic field at the perforated position (or rims), which is the result of symmetry breaking in silver nanocap array. The theoretical study about perforated nanoshells by Wang *et al.*[5] indicated that the hybridization between sphere-like and void-like surface plasmon leads to the enhancement of intense local electromagnetic field. It is also noted that the fluorescence background of R6G molecules, which always exists in SERS measurement (the inset of Fig. 4(a)) and obscures calibration and quantization of spectral peak information,[20] is highly suppressed as the R6G molecules are absorbed into the perforated silver nanocap array. To investigate the uniformities and reproducibilities of the fabricated silver nanocap arrays, the SERS spectra taken from 9 different positions in an area of 3 μm × 3μm, separately, on the imperforated and perforated arrays are shown in Figs. (a2) and (a3) (See items (a2) and (a3) in Appendix A) respectively, and the spot-to-spot variations of characteristic SERS peak (1364 cm^{-1}) intensity for both silver nanocap arrays, shown in Figs. (a4) and (a5) (See items (a4) and (a5) in Appendix A), are below 10%, which indicates that the uniformities and reproducibilities of both imperforated and perforated nanocap arrays are excellent.

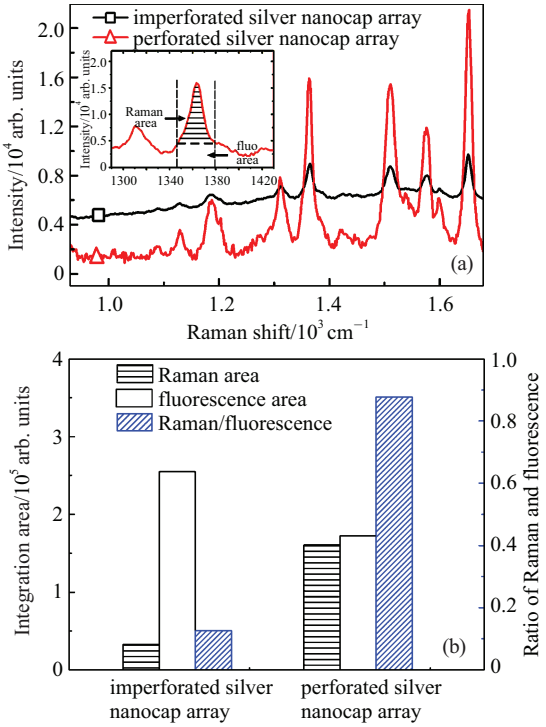


Fig. 4. (color online) (a) SERS spectra of R6G with 514-nm excitation for imperforated (curve with square) and perforated silver nanocap array (curve with triangle), where the inset shows the fluorescence background below the characteristic SERS peak (1364 cm^{-1}). (b) Comparisons of SERS activity (denoted by characteristic Raman area), fluorescence suppression (denoted by fluorescence area) and the ratios of Raman and fluorescence background between imperforated and perforated silver nanocap arrays.

4. Conclusions

In this paper, we proposed a novel perforated silver nanocap array with high SERS activity and fluorescence suppression. The array was fabricated by electron beam evaporating Ag onto the perforated barrier layer side of an HA AAO template. The analyses of morphology and optical property reveal that the fabricated perforated silver nanocap array exhibits both reduced symmetry and metallic ordered characteristics. The results of SERS experiments indicate that the perforated silver nanocap array promises potential applications in sensitive SERS with fluorescence suppression.

Appendix A

(a1) Supporting information about EDS analysis of the perforated silver nanocap array (Fig. (a1)).

(a2) Supporting information about SERS spectra taken from 9 different positions on imperforated silver nanocap arrays (Fig. (a2)).

(a3) Supporting information about SERS spectra taken from 9 different positions on perforated silver nanocap arrays (Fig. (a3)).

(a4) Supporting information about the variations in characteristic SERS peak (1364 cm^{-1}) intensity of the imperforated silver nanocap arrays (Fig. (a4)).

(a5) Supporting information about the variations in characteristic SERS peak (1364 cm^{-1}) intensity of the perforated silver nanocap arrays (Fig. (a5)).

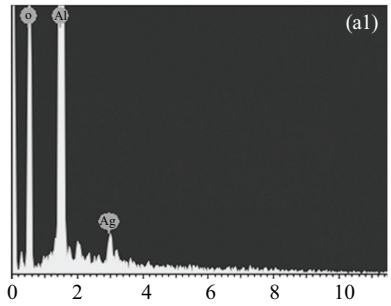


Fig. (a1).

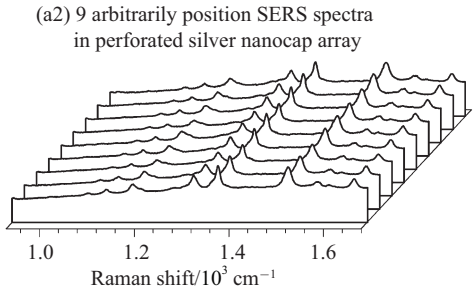


Fig. (a2).

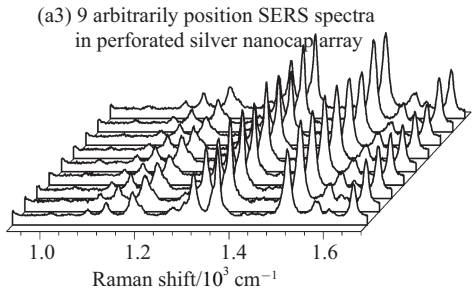


Fig. (a3).

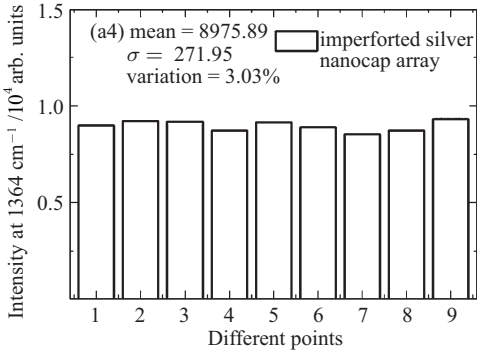


Fig. (a4).

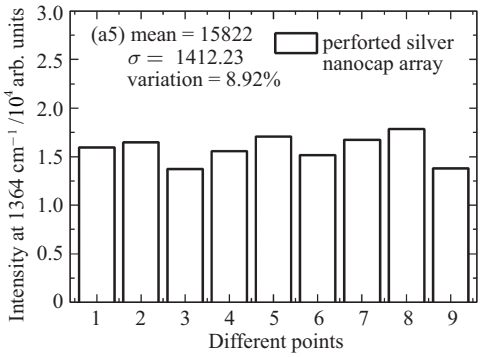


Fig. (a5).

References

[1] Knight M W and Halas N J 2008 *New J. Phys.* **10** 105006
[2] Mirin N A and Halas N J 2009 *Nano Lett.* **9** 1255
[3] Van Dorpe P and Ye J 2011 *ACS Nano* **5** 6774
[4] Mirin N A, Ali T A, Nordlander P and Halas N J 2010 *ACS Nano* **4** 2701
[5] Wang Q G, Tang C J, Chen J, Zhan P and Wang Z L 2011 *Opt. Express* **19** 23889
[6] Lu Y, Liu G L, Kim J, Mejia Y X and Lee L P 2005 *Nano Lett.* **5** 119
[7] Hao F, Sonnefraud Y, Dorpe P V, Maier S A, Halas N J and Nordlander P 2008 *Nano Lett.* **8** 3983
[8] Lee W, Ji R and Nielsch K 2006 *Nat. Mater.* **5** 741
[9] Zhang X F and Fang Y 2006 *Acta Phys. Sin.* **55** 3785 (in Chinese)
[10] Huang L Q, Pan H Q, Wang J, Tong H M, Zhu K, Ren G X and Wang Y C 2007 *Acta Phys. Sin.* **56** 6712 (in Chinese)
[11] Wang H H, Liu C Y, Wu S B, Liu N W, Peng C Y, Chan T H, Hsu C F, Wang J K and Wang Y L 2006 *Adv. Mater.* **18** 491
[12] Wang J, Huang L Q, Yuan L, Zhao L H, Feng X H, Zhang W W, Zhai L P and Zhu J 2012 *Appl. Surf. Sci.* **258** 3519
[13] Du Y, Shi L, He T, Sun X and Mo Y 2008 *Appl. Surf. Sci.* **255** 1901
[14] Lang X, Qiu T, Zhang W, Yin Y and Chu P K 2011 *J. Phys. Chem. C* **115** 24328
[15] Fu S L, Li H J, Xie S X, Zhou X, Xu H Q and Xia H 2011 *Chin. Phys. B* **20** 087302
[16] Shi X Z, Shen C M, Wang D K, Li C, Tian Y, Xu Z C, Wang C M and Gao H J 2011 *Chin. Phys. B* **20** 076103
[17] Han C Y, Willing G A, Xiao Z and Wang H H 2007 *Langmuir.* **23** 1564
[18] Lillo M and Losic D 2009 *J. Membrane Sci.* **327** 11
[19] Watanabe H, Hayazawa N, Inouye Y and Kawata S 2005 *J. Phys. Chem. B* **109** 5012
[20] Farcau C and Astilean S 2011 *Chem. Commun.* **47** 3861